

the desired gradient. In Fig. 12b, the turbine is 10% overdesigned. In this case there is enough torque available to allow the pressure to follow its desired gradient. Temperature again follows its desired response quite well. The same gains on the controllers are used as for the controlled system for critical starts ($G_1 = 10$, $G_2 = 10$, $G_3 = 0.008$). For these subcritical starts the initial control-rod settings are not equal to their design values but are slightly lower. This reduction in control-rod reactivity is cancelled by the integral feedback controller of the control rods after the transients have been completed. The performance of the controlled, initially subcritical system is then very similar to that of the controlled critical system.

Controlled Change in Design Point Operation

For sudden increases of the desired pressure, when the system is in operation, an excursion of the power level and consequently a change in temperature can be expected. The turbine must be overdesigned to bring the pressure a certain percentage over its design value. The system behavior for a change in desired pressure shows that the resultant temperature excursion is a much smaller percentage of its design point value than the percentage change in design pressure. For example, a 10% increase in pressure results in a temperature

excursion of 2.5%, whereas a 20% increase in pressure results in a temperature excursion of 4%.

References

- ¹ Mohler, R. R. and Perry, J. E., Jr., "Nuclear rocket engine control," *Nucleonics* 19, 80 (April 1961).
- ² Hess, G. K., Jr., Demuth, H. B., Brown, E. A., and Mohler, R. R., "Control systems for the KIWI-A nuclear reactor rocket engines," *Inst. Radio Engrs. International Symposium, Las Vegas, Nev.* (October 25, 1961).
- ³ "Starting and control characteristics of nuclear rocket engines," Northern Research and Engineering Corp. Rept. 1034-2 (February 1961).
- ⁴ Yoshitani, Y., "The thermal performance of homogeneous graphite reactors," *Mass. Inst. Tech. S. M. Thesis* (June 1960).
- ⁵ Felix, B. R., "Dynamic analysis of a nuclear rocket engine system," *ARS J.* 29, 853-862 (1959).
- ⁶ Smith, H. P., "Closed loop dynamics of nuclear rocket engineering with bleed turbine drive," *Nucl. Sci. Eng.* (to be published).
- ⁷ Smith, H. P. and Stenning, A. H., "Dynamics and control of nuclear rocket engines," *Nuclear Eng. Dept., Mass. Inst. Tech., Contract DSR8246, performed for Pratt & Whitney Div., United Aircraft Corp.* (August 1960).
- ⁸ Schultz, M. A., *Control of Nuclear Reactors and Power Plants* (McGraw-Hill Book Co. Inc., New York, 1955), Chap. 11.

Liquid Injection Thrust Vector Control

C. J. GREEN* AND FOY McCULLOUGH JR.†

U. S. Naval Ordnance Test Station, China Lake, Calif.

The technique of obtaining thrust vector control by the injection of liquid into the supersonic region of a rocket nozzle has been studied. This paper presents the experimental results obtained with various liquid injectants together with the effects of some of the more critical physical parameters. Liquids studied were water, Freon-12, perchloroethylene, nitrogen tetroxide, and bromine. In addition, unsymmetrical dimethylhydrazine and inhibited red fuming nitric acid were injected simultaneously to explore the effect of energy release in the nozzle exit cone with bipropellant injection. Data on the relationships of side force to injectant flow rate, the effect of axial location of the injection port, the effect of injection pressure, and the effects of injection properties are presented and discussed.

Nomenclature

A	= injection port area, in. ²
F_m	= main thrust, lb
F_s	= side thrust, lb
g	= gravitational constant, ft/sec ²
I_{sp}	= specific impulse (motor), sec
\dot{W}_c	= main propellant flow rate, lb/sec
\dot{W}_s	= secondary flow rate, lb/sec
ρ	= injectant density, lb/ft ³
V_s	= injectant velocity, fps
C_V	= velocity coefficient
Δp	= injection pressure, psi

Received by ARS March 9, 1962; revision received December 10, 1962.

* Aerospace Engineer (Propulsion and Power), Test and Evaluation Division, Propulsion Development Department.

† Head, Test and Evaluation Division, Propulsion Development Department. Member AIAA.

AS the performance of propulsion systems increases, accompanied in most cases by increased combustion temperatures, the problem of satisfactory materials for mechanical thrust-vector-control devices becomes increasingly critical. With this problem in mind, a study of possible techniques of thrust vector control was initiated at the Naval Ordnance Test Station in 1958.¹ The technique of injecting a fluid into the expansion cone of a supersonic nozzle (secondary injection) to produce a usable side force or thrust vector force appeared to be the most promising new technique (Fig. 1).

The initial studies of secondary injection²⁻⁶ used gases as the injected fluids. These studies, in general, indicated that for maximum effectiveness the injected gas should be near the combustion temperature of the mainstream gases. To avoid the high temperature materials problems and to facilitate system design and development, the use of liquids as injectants was proposed. The feasibility of using liquids was demonstrated early in 1959.⁷

Experimental Procedures

Both liquid and solid propellant motors were used in this experimental program. One injection test was conducted using a solid propellant motor loaded with B. F. Goodrich E-107 polyurethane propellant containing 17.7% aluminum by weight. The remainder of the tests were conducted with the liquid propellant applied research motor (LPARM).

LPARM Injection Tests

For the work reported in this paper, the LPARM was operated with unsymmetrical dimethylhydrazine and inhibited red fuming nitric acid at the following nominal conditions: thrust, 3500 lb; chamber pressure, 1200 psi; expansion ratio, 12:1; and I_{sp} , 200 sec.

The test nozzles (Figs. 2 and 3) were uncooled and used graphite throat inserts. These nozzles were adequate for tests of 3 to 4 sec duration. The 16-point nozzle (Fig. 2) was fabricated with four rows of four orifices 90° apart. Each row of orifices was drilled a different diameter. This arrangement permitted the effect of orifice area and axial location of the injection port to be studied. All orifices were round and were drilled perpendicular to the nozzle axis. During most tests, injection pressures and flow rates were varied through the use of a hydraulically controlled metering valve. For the bipropellant injection tests, the basic nozzle body was modified to permit the insertion of bipropellant injectors (Fig. 3).

Side-force measurements were obtained through the use of a pivot mount, lever arm, and force transducer. The side-force assembly was fastened in turn to a flexure mount to permit the measurement of axial thrust (Fig. 4). All side-force measurements reported are resolved to a point on the nozzle 6.42 in. from the throat. Calibration of both side-force and axial thrust was accomplished "in place" through the use of proving rings.

Solid Motor Injection Test

This test was conducted primarily for purposes of data comparison. The effects of different motor performances and of the aluminized propellant were of particular interest. In addition, three different injection geometries were investigated. Figure 5 depicts the nozzle used in this test. The performance characteristics of this motor are as follows: thrust, 3635 to 2835 lb; chamber pressure, 1115 to 855 psi; specific impulse, 237 sec; expansion ratio, 8.15:1; and burn time, 35 sec.

Both Freon-12 and nitrogen tetroxide were used as injectants. Nitrogen tetroxide was injected through a single orifice only, and Freon-12 was injected through both single and multiple orifice configurations.

The fluids were injected in a cyclic fashion during the first 26 sec of the 35-sec motor burning time. An attempt to vary the flow rate of each injectant by a "blow-down" technique was only partially successful.

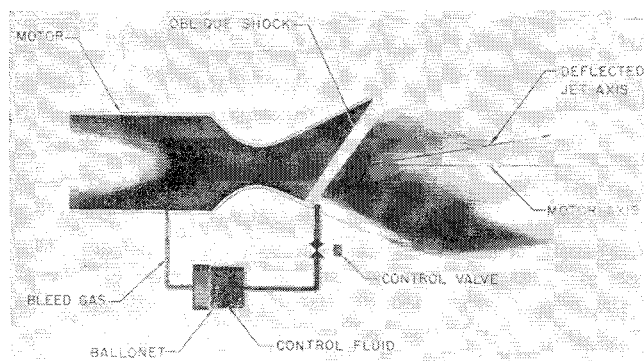


Fig. 1 Thrust vectoring by secondary injection

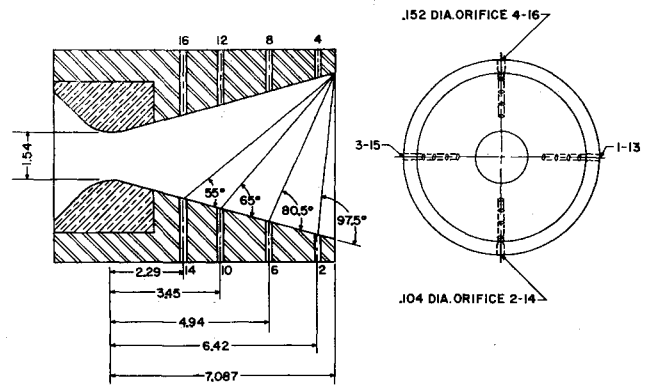


Fig. 2 Sixteen-point nozzle

Side-force was measured in two planes 90° apart. All side-forces are resolved to the nozzle exit plane.

Results

Seven liquids, including UDMH and IRFNA, were used as injectants in this experimental program. The five fluids used individually were Freon-12, perchloroethylene, water, bromine, and nitrogen tetroxide. The data are presented graphically in the form of the ratio of side force to main thrust vs the ratio of secondary flow rate to main flow rate. The position numbers noted on each graph refer to the axial location and size of the injection port. In some cases, fluids were injected through two orifices located in-line axially. Consequently, the notation on the graph specifies two position numbers.

The nominal motor characteristics provided previously may be considered descriptive of the motor conditions under which the presented data were obtained. Detailed test data such as flow rate, injection pressure, chamber pressure, thrust level, etc., are provided in data tabulations.⁹

LPARM Data

Freon-12 Injection

The family of curves shown in Fig. 6 represents the results obtained by injecting Freon-12 at four different axial locations through orifices 0.152 in. in diameter. The effect of variations in axial location is quite apparent.

Figure 7 shows the results of Freon-12 injected through 0.104-in.-diam orifices at four different axial locations. Injection pressure for this case is considerably higher than for the 0.152-in.-diam orifices at similar weight flow ratios. The effect of axial location is consistent with the large diameter orifice results. Comparing the results of position 10 and 12, 6 and 8, and 2 and 4 (identical axial locations), it may be seen that the smaller orifice provides better performance. This performance increase is greater than that to be expected from the contribution of a higher product of injectant mass flow rate and velocity. No improvement in per-

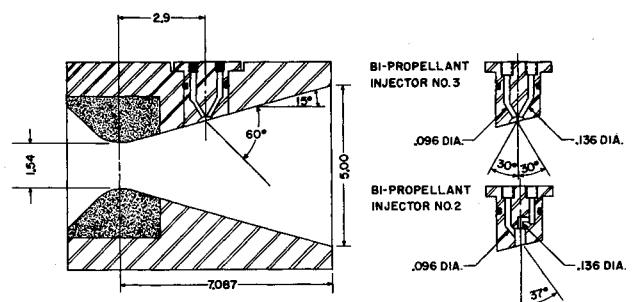


Fig. 3 Bipropellant injection nozzle

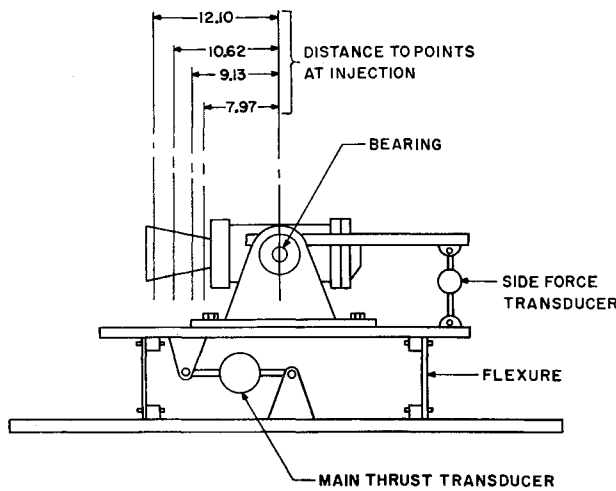


Fig. 4 Schematic of LPARM motor mount

formance is apparent in comparing the results from position 14 and 12.

Figure 7 also shows the results obtained by injecting Freon-12 through two orifices (0.104-in.-diam) located in-line axially. The performance obtained is approximately equivalent to injection through a single orifice of an equivalent total area, and lower than that obtained with a single 0.104-in.-diam orifice.

Perchloroethylene Injection

Figures 8 and 9 show the results obtained by injecting perchloroethylene through 0.152- and 0.104-in.-diam orifices at various axial locations. The effect of axial location and injection pressure is consistent with the Freon-12 data in all cases. The double orifice injection (Fig. 9, positions 10 and 14) gave results lower than a single orifice of one half the effective area and gave results approximately equivalent to a single orifice with an equivalent total area (Fig. 8).

Water Injection

Figure 10 shows the results obtained from water injection through one 0.152-in.-diam orifice (position 12) and through two 0.152-in.-diam orifices (positions 16 and 12). Double orifice injection again shows a reduction in performance when compared to a single circular orifice of one half the effective area.

Bipropellant Injection

Figure 11 shows the results obtained from the simultaneous injection of UDMH and IRFNA. The object of the tests was to determine the effects of any exothermic reaction of the injectant within the expansion cone. Two injector designs were used for these tests (Fig. 3); both designs yielded approximately the same results. Bipropellant injection provided the highest performance ratio obtained in this test

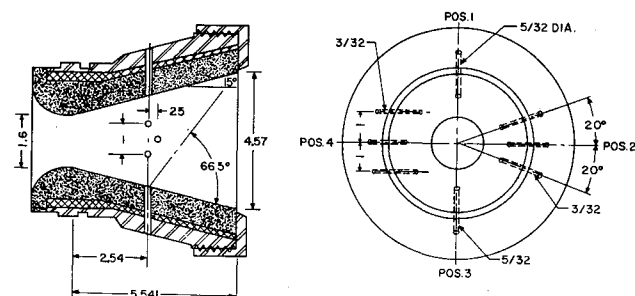


Fig. 5 Solid motor test nozzle

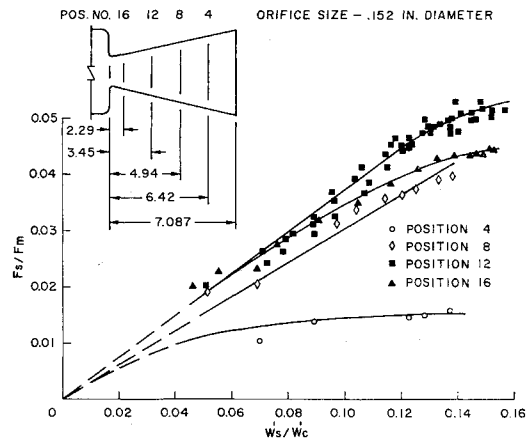


Fig. 6 Freon-12 injection data

series. Secondary O/F ratio and injector design had no apparent effect upon performance. Secondary O/F ratio varied between 0.975 and 3.8.

Bromine Injection

Only two data points were obtained for bromine. These points are presented in Fig. 11 with the bipropellant injection data.

Solid Motor Injection Data

Figure 12 is a summary of data obtained from the injection tests with the solid propellant motor. Both Freon-12 and nitrogen tetroxide were used as injectants for this test. Nitrogen tetroxide was injected through a single orifice only, and Freon-12 was injected through both single and multiple orifice configurations (Fig. 5). In Fig. 6, "Freon-12 radial" and "Freon-12 parallel" refer to positions 2 and 4, respectively, in Fig. 5. Main propellant flow rates were obtained by dividing the main thrust by the propellant specific impulse. The propellant specific impulse was assumed to remain constant over the test duration.

Discussion

Relation of Side Thrust to Injectant Flow Rate

Fixed area orifices were used for all injection tests in this program. Consequently, injectant flow rate was varied by changing injection pressure (variable pressure injection). Under these injection conditions, the variation in side thrust

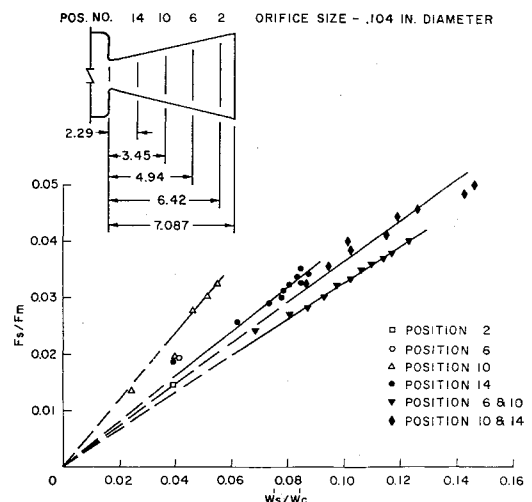


Fig. 7 Freon-12 injection data

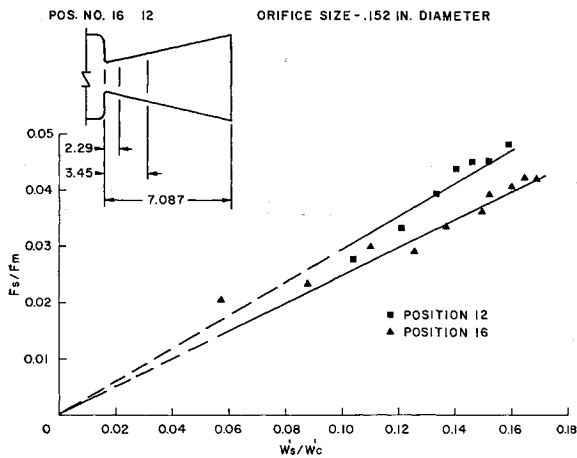


Fig. 8 Perchloroethylene injection data

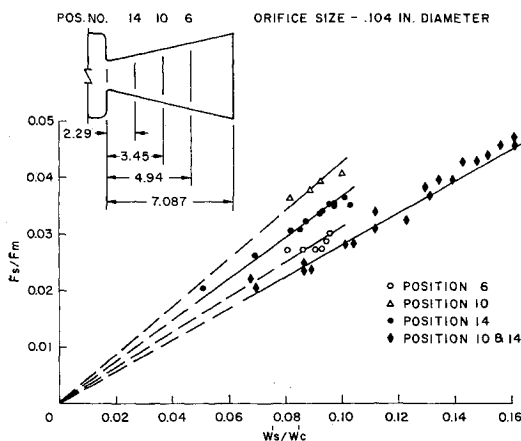


Fig. 9 Perchloroethylene injection data

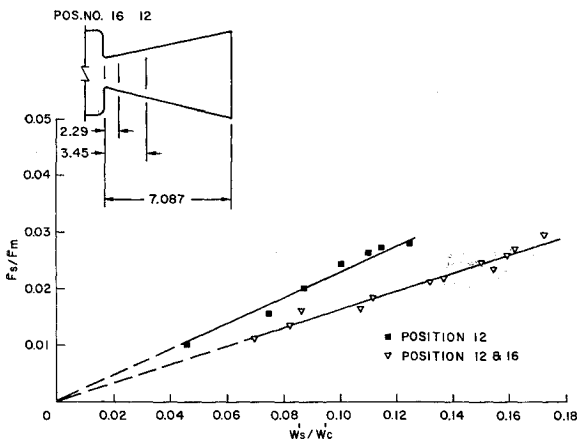


Fig. 10 Water injection data

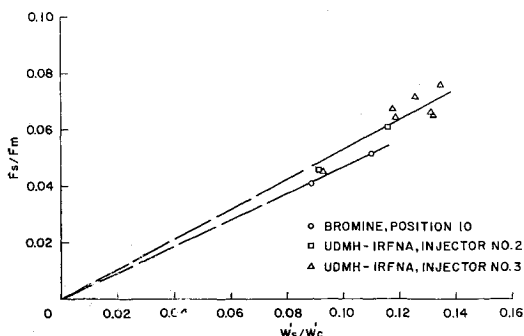


Fig. 11 Bipropellant and bromine injection data

with secondary flow rate was found to be essentially linear for near optimum axial locations; i.e., the injectant specific impulse was found to be constant. The slope of the line describing the data has been termed the performance ratio of the fluid ($F_s/\dot{W}_s \div F_m/\dot{W}_c$). In comparing the results of variable pressure injection for ports of different areas (different injection pressures at similar flow rates), it is noted that variations in the performance ratio of a single injectant are obtained.

Thus, if injectant flow rates were varied via a variable area orifice (constant pressure injection), a nonlinear relation between side force and flow rate would be expected.

The solid propellant test data indicate a tendency for the performance ratio of an injectant to remain constant with changes in motor performance. Thus, injectant specific impulse (F_s/\dot{W}_s) or performance is increased when motor performance is increased.

Effects of Axial Location

The test data indicate an optimum axial location for maximum injectant performance, which is dependent upon injectant flow rate. The LPARM data indicate that injectant performance increases, for secondary flow rates of 5 to 15% through a 0.152-in.-diam orifice, as the injection port is moved upstream to a point approximately 3.5 in. from the throat. As secondary flow rates exceed approximately 13% of main propellant flow rate at position 12, the performance ratio of Freon-12 appeared to decrease. It is believed that this reduction of the performance ratio of an injectant at high flow rates may be attributed to extreme radial dispersion of the pressure field causing side-force or reflection of the shock wave off the wall opposite the injection port. In either case, the integration of the radial components of the pressure area forces can yield a decreased component of side-force. Data obtained from the three-port parallel orifice configuration (Fig. 5) indicate a reduction of the performance ratio of the injectant. This reduction was probably due to the radial spread of the pressure field. The three-port radial configuration, on the other hand, showed an increase in the performance ratio over the single-port configuration, indicating that some radial spread may be desired, probably due to the increase in mixing efficiency and heat transfer.

Some success in describing the optimum injector location has been experienced by considering the maximum possible oblique shock angle that can be generated in the nozzle. Equating this angle with the included angle described by the wall of the nozzle and a line from the injection port to a point on the opposite wall at the exit plane (Fig. 2) approximates the optimum location.

Effect of Orifice Area or Injection Pressure

Variations in the performance ratio of a single injectant have been noted when the area of the injection port is changed. The data presented in this report indicate a relation between the rate of change of momentum of the injected fluid to the side thrust developed. The ratio F_s/F_m has been plotted vs $\dot{W}_s^2/g\rho A$ (rate of change of injectant momentum or thrust). This tended to group the data as shown in Fig. 13. The contribution of injectant thrust to total side force is not sufficient to account for the observed increase in performance associated with higher injectant pressures. Consequently, it was postulated that the rate of change of injectant momentum had additional influence in that its magnitude would effect the degree of penetration of the exhaust stream by the injectant fluid, thereby influencing injectant vaporization and mixing, etc. In addition, the degree of penetration was considered to be a function of the exhaust stream rate of change of momentum. The foregoing considerations led to the hypothesis that the ratio of side-force to main thrust was a function of the ratio of the rate of change of momentum

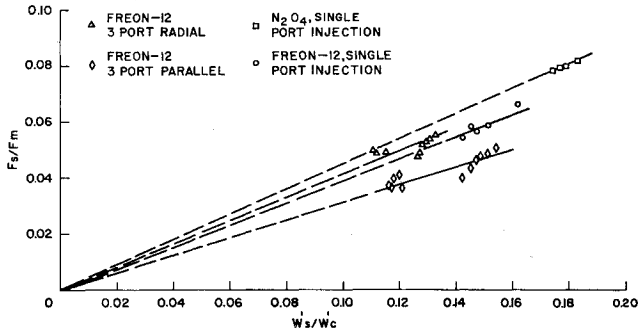


Fig. 12 Solid propellant motor, injection test data

of the secondary and primary streams. Consequently, the ratio F_s/F_m has been plotted as a function of $\dot{W}_s^2/\dot{W}_c^2 \div g\rho A$ (Fig. 14). The term $\dot{W}_s^2/\dot{W}_c^2 \div g\rho A$ is representative of a rate of change of momentum ratio (although it does have dimensions), as the rate of change of momentum of the exhaust gases is proportional to \dot{W}_c^2 . The data now are seen to fall into distinct groups. Data on injection through two different sizes of orifices, and even for simultaneous injection through two orifices in line axially, appear to lie on essentially a single straight line when plotted on log paper. The data for these graphs were obtained from graphs of F_s/F_m vs \dot{W}_s/\dot{W}_c for similar axial locations. Figure 15 shows points of equivalent secondary flow rates through various orifice diameters. From this arrangement of data, it may be seen that injection pressure should be as high as possible for a given flow rate. From the averaged curves in Fig. 15, approximate equations describing the injection of the various fluids may be obtained. These equations will take the form of

$$F_s/F_m = C_0[\dot{W}_s^2/\dot{W}_c^2 \div g\rho A]^{1/2}$$

A more suitable form of the foregoing equation may be developed in the following fashion:

rate of change of injectant momentum =

$$\dot{m}_s V_s = (\dot{W}_s/g) C_V [2g \Delta p/\rho]^{1/2} \text{ lb}$$

rate of change of exhaust gas momentum =

$$\dot{W}_c I_{sp} \text{ lb}$$

if

$$F_s/F_m = \text{const}[\dot{m}_s V_s/\dot{W}_c I_{sp}]^{1/2}$$

and, therefore,

$$\left[\frac{\dot{m}_s V_s}{\dot{W}_c I_{sp}}\right]^{1/2} = \left[\frac{\dot{W}_s}{\dot{W}_c}\right]^{1/2} \left[\frac{C_V [2g \Delta p/\rho]^{1/2}}{g I_{sp}}\right]^{1/2}$$

then

$$\frac{F_s}{F_m} = C_2 \left[\frac{\dot{m}_s V_s}{\dot{W}_c I_{sp}}\right]^{1/2} = C_1 \left[\frac{\dot{W}_s}{\dot{W}_c}\right]^{1/2} \left[\frac{1}{I_{sp}}\right]^{1/2} (\Delta p)^{1/4}$$

The solid motor test and results of subsequent testing not presented here have indicated that the product of $C_1(1/I_{sp})^{1/2}$ tends to be a constant; i.e., injectant performance ratio remains constant with varying motor performance. Thus,

$$F_s/F_m = C(\dot{W}_s/\dot{W}_c)^{1/2}(\Delta p)^{1/4}$$

where C is an empirical dimensional constant.

This relation has been used effectively to apply and correlate data over a wide range of conditions (thrust levels of 3500 to 35,000, I_{sp} from 200 to 255 sec, and secondary to primary weight flow ratios of 0.04 to 0.4).¹⁰

Constant pressure injection by means of a variable area orifice or orifices will influence system design considerably if only small corrective forces are required for the major portion of the flight time, and large corrective forces are re-

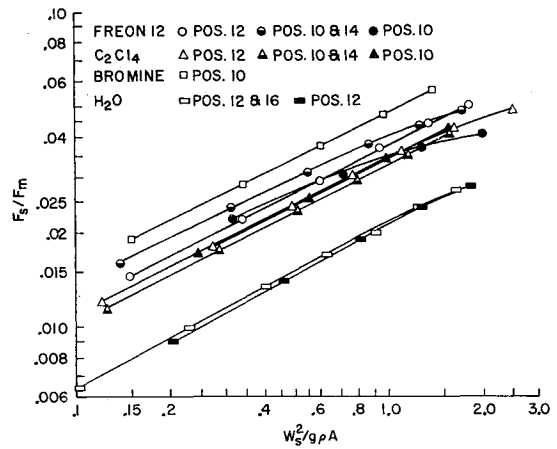


Fig. 13 Force ratio vs rate of change of injectant momentum

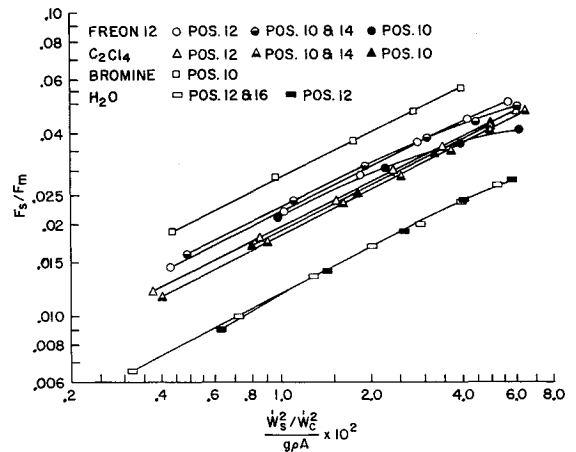


Fig. 14 Force ratio vs rate of change of injectant momentum/(chamber flow rate)²

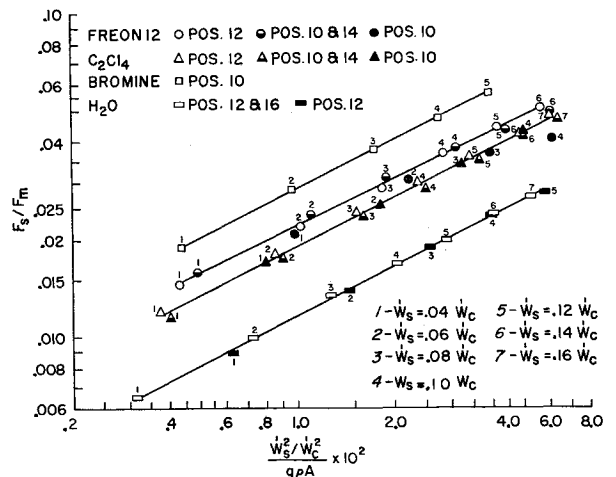


Fig. 15 Force ratio vs rate of change of injectant momentum/(chamber flow rate)²

quired intermittently. Total fluid weight required to deliver a given lateral impulse may be reduced by a factor of 1.5 to 2 (depending upon the relative magnitudes of the maximum required side force, and the average side forces) through the use of variable area valving as opposed to constant pressure valving. The use of the foregoing empirical expression, relating the ratio of side-force and main thrust to the ratio of secondary flow rate and primary flow rate and injection pressure, allows the approximation of fluid weight required

(for either variable pressure injection, variable area injection, or any combination of the two) if the schedule of required vehicle turning moment vs time is known and if a subscale data point is available. This expression has been used extensively with Freon-12, perchloroethylene, Freon-113, and Freon-114B-2. The subscale conditions must simulate the full scale conditions insofar as injection angle, number of orifices (and geometrical arrangement), axial location, and nozzle half angle are concerned.

Effect of Injectant Characteristics

The total side-force resulting from the injection of a fluid into the expansion cone of a rocket nozzle may be considered to consist of two components: 1) a component of side-force due to the thrust of the fluid upon injection (product of mass flow rate and velocity plus a pressure area term for gas injection), and 2) a component due to the interaction of the injected fluid with the mainstream gases. The second component consists of a static pressure recovery of the mainstream gases acting over an asymmetrical area within the nozzle. The pressure area force resulting from this pressure recovery represents from 80 to 90% of the total developed side-force in the case of liquid injection.

A one-dimensional model of this fluid interaction process has been analyzed.⁸ The results of this analysis indicate that the injectant should provide as large an obstruction as possible to mainstream flow and should react or decompose with a release of heat or, in the case of an inert fluid, vaporize and/or dissociate with a minimum amount of heat absorption. Consequently, the following, and in some cases conflicting, injectant characteristics are desired: 1) low specific heat in liquid and vapor phases, 2) low boiling point, 3) low heat of vaporization, 4) high heat of reaction or exothermic decomposition, 5) low molecular weights of products of combustion or decomposition, and 6) high density (from a packaging standpoint).

References

- ¹ Bankston, L. T., "Thrust vectoring methods," U. S. Naval Ordnance Test Station, China Lake, Calif., NAVORD Rept. 6423, NOTS 2123 (December 2, 1962); confidential.
- ² Hausmann, G. F., "Thrust axis control of supersonic nozzles by airjet shock interference," United Aircraft Corp., Hartford, Conn., Research Dept. Rept. R-63143-24 (May 2, 1952); confidential.
- ³ Schulmeister, M., "Static evaluation tests of an oblique shock wave system for rocket exhaust deflection," U. S. Naval Air Rocket Test Station, Lake Denmark, Dover, N. J., NARTS 77, TED-ARTS-S1-5519 (December 1955); confidential.
- ⁴ Schweiger, M. K., "Jet induced thrust vector control applied to nozzles having large expansion ratios," United Aircraft Corp., Hartford, Conn., Research Dept. Rept. R-0937-33 (March 1, 1957); confidential.
- ⁵ Bankston, L. T. and Larsen, H. M., "Thrust vectoring by secondary injection in the nozzle exhaust cone," Bull. 15th Meeting, JANAF, Solid Propellant Group, Silver Spring, Md., SPIA 7, 151-169 (June 1959); confidential.
- ⁶ Bankston, L. T. and Larsen, H. M., "Thrust vectoring experiments: gas injection," U. S. Naval Ordnance Test Station, China Lake, Calif., NAVORD 6548, NOTS 2247 (May 28, 1959).
- ⁷ McCullough, F., Jr., "Thrust vector control by secondary injection," *Proceedings of the Symposium on Ballistic Missile and Space Technology* (Space Technology Labs., Los Angeles, Calif., 1959), Vol. 1, pp. 1-25; confidential.
- ⁸ Green, C. J. and Benham, C. B., "Parameters controlling the performance of secondary injection," U. S. Naval Ordnance Test Station, China Lake, Calif., NAVWEPS 7743, NOTS 2710 (December 1961).
- ⁹ Green, C. J. and McCullough, F., Jr., "Liquid injection thrust vector control," U. S. Naval Ordnance Test Station, China Lake, Calif., NAVWEPS 7744, NOTS 2711 (June 16, 1961).
- ¹⁰ Benham, C. B., "The design, development and test of a liquid-injection thrust-vector-control system for the Polaris A-3 second-stage motor," U. S. Naval Ordnance Test Station, China Lake, Calif., NAVWEPS 7969, NOTS 3019 (to be published); confidential.

MARCH 1963

AIAA JOURNAL

VOL. 1, NO. 3

Shock-Induced Boundary Layer Separation in Overexpanded Conical Exhaust Nozzles

M. ARENS* AND E. SPIEGLER†

Technion-Israel Institute of Technology, Haifa, Israel

The flow in overexpanded supersonic nozzles is reviewed. Although five essentially different flow regimes can be discerned, depending on the nozzle pressure ratio, the regime of most interest to the engine designer is the one characterized by oblique shock patterns in the nozzle and flow separation from the nozzle wall. It is shown that the pressure rise associated with the separation correlates well with the Mach number at the separation point. A simple analytical formulation for the pressure rise required to separate the flow provides excellent agreement with experimental data over a wide range of nozzle operating conditions and allows prediction of overexpanded nozzle performance.

Nomenclature

M = Mach number
 p = pressure

u = velocity
 α = nozzle half angle
 γ = specific heat ratio
 δ = flow deflection angle

Subscripts and superscripts

a = ambient
 b = origin of separated region
 c = stagnation at nozzle entry
 s = origin of shock wave-boundary layer interaction
 $*$ = characteristic velocity

Received by ARS August 28, 1962; revision received December 12, 1962. This research was supported in part by the Gerard Swope Fund.

* Associate Professor, Department of Aeronautical Engineering.

† Graduate Assistant, Department of Aeronautical Engineering.